J Fluoresc (2012) 22:485–494
DOI 10.1007/s10895-011-0982-4

ORIGINAL PAPER

Analysis of Lanthanide-Induced Conformational Change of the C-Terminal Domain on Centrin

Ya-Qin Zhao · Jun Yan · Li Song · Ya-Nan Feng · Ai-Hua Liang · Bin-Sheng Yang

Received: 20 December 2010 / Accepted: 16 September 2011 / Published online: 27 September 2011

Abstract Centrin, an EF-hand calcium-binding protein with high homology to calmodulin (CaM), is an essential component of microtubule-organizing center (MTOC). Lanthanide (Ln) ions can improve the stability, increase the amount and enhance the orderliness of microtubules, which are components of cytoskeleton. In order to investigate the structural basis of Ln ions on enhancing orderliness of microtubules, we characterized the binding properties of Ln ions with the isolated C-terminal domain of the *Euplotes* centrin (C-EoCen). Results suggested that Ln ions may occupy the canonical Ca^{2+} binding sites on C-EoCen with middle affinity. Near- and far-UV CD spectra of C-EoCen displayed pronounced differences before and after additing Ln ions. The asymmetry of microenvironments of Phe on C-EoCen was changed. Using 2-*p*-toluidinylnaphthalene-6- sulfonate (TNS) as probe, Ln ions induced C-EoCen to undergo conformational changes from closed state to open state, resulting in exposing hydrophobic patches to external environments. Ln ions have more obvious effect on the conformation of centrin than Ca^{2+}. The differences found in the interactions of centrin binding with Ln ions/Ca^{2+} maybe provide some insights for structural basis of centrin functions in vivo.

Keywords Centrin · Lanthanide ions · Conformational change

Abbreviations

MTOC	Microtubule-organizing centers
EoCen	*Euplotes octocarinatus* centrin
C-EoCen	C-terminal domain of *Euplotes octocarinatus* centrin
PAGE	Polyacrylamide gel electrophoresis
SPB	Spindle pole body
RLS	Resonance light scattering
CaM	Calmodulin
EDTA	Disodium ethylenediaminetertraacetic
Hepes	N-2-hydroxyethylpiperazine-N-2-ethanesulfonic acid
XO	3,3′-bis[*N,N'*-bis(carboxymethyl) aminomethyl]-*o*-cresolsufonphthalein
TNS	2-*p*-toluidinylnaphthalene-6-sulfonate
IPTG	Isopropyl-β-D-thiogalactopyranoside
CD	Circular dichroism

Introduction

Centrin, also known as caltractin, is one of the conserved components of microtubule organizing center (MTOC) [1]. It belongs to the EF-hand superfamily of calcium-binding proteins. This protein has been identified in diverse higher and lower organisms including yeast, ciliates, green algae, higher plants, invertebrates, and vertebrates [2, 3]. Accumulating evidences demonstrate that centrin is responsible for Ca^{2+}-dependent motility processes, at least in ciliated or flagellate cells [4]. And other functions were also discovered, including signal transduction [2, 5], proper cellular division

Electronic supplementary material The online version of this article (doi:10.1007/s10895-011-0982-4) contains supplementary material, which is available to authorized users.

Y.-Q. Zhao · J. Yan · Y.-N. Feng · B.-S. Yang (✉)
Key Laboratory of Chemical Biology and Molecular Engineering of Ministry of Education, Institute of Molecular Science, Shanxi University,
Taiyuan 030006, China
e-mail: yangbs@sxu.edu.cn

L. Song · A.-H. Liang
Institute of Biotechnology, Shanxi University,
Taiyuan 030006, China

[6], initiation of flagella excision [7], forming complex for the recognition of damaged DNA [8], modulation of homologous recombination and nucleotide excision repair [9], involvement with nuclear mRNA export [10], fibers contraction [2, 5] and the activity of voltage-gated Ca^{2+} channels in *Paramecium* [11]. Comparative analysis of centrin protein sequences revealed that they are closely related to the ubiquitous archetypal EF-hand calcium sensor protein calmodulin (CaM), a calcium-regulating on/off switch. Like CaM, centrin consists of two structurally independent globular domains connected by a flexible linker. Both the N- and the C-terminal halves exhibit significant Ca^{2+} affinity and undergo metal-induced conformational changes, which may have a physiological relevance. Each structural domain contains two helix-loop-helix (known as EF-hand) Ca^{2+}-binding motifs [1, 12]. The 12-residue loop is responsible for the binding and coordination of the metal ions in the EF-hand loops. The Ca^{2+} ion is coordinated to seven oxygen ligands: monodentate carboxylate or carboxamide ligands are in positions 1, 3, and 5 of the loop, a backbone carbonyl ligand is in position 7, and a universally conserved glutamate is in position 12. The γ-carboxylate of this glutamate coordinates to the Ca^{2+} ion in a bidentate manner, i.e., using both carboxylate oxygen atoms. A water molecule generally provides the seventh oxygen ligand for the Ca^{2+} ion. Having similar ion radii and coordination numbers, lanthanides (Ln) ions may substitute Ca^{2+} in this EF-hand proteins and exhibit higher affinities for proteins [13]. Numerous results have been reported papers concerning the effects of Ln ions on CaM [14–16]. *Via* Ca^{2+}-dependent interactions with dozens of known cellular targets, CaM involves in a wide range of cellular process and functions the biological effects of Ln ions [17]. Due to their high homology and identical domain architecture between centrin and CaM, it is conceivable that the biological effects of Ln ions may, at least partially, results from the interaction of Ln with centrin. However, few investigations about the conformational effect of Ln ions apart from Tb^{3+} on centrin have been focused on.

The Ciliate *Euplotes octocarinatus* centrin (EoCen) was first cloned by our group (GenBank accession number: Y18899). It belongs to the EF-hand Ca^{2+}-binding protein family and contains 168 residues. EoCen has four Ca^{2+}-binding sites (designated sites I-IV), apart from Ca^{2+} which can also bind with Tb^{3+} with association constants (K_a) in the range $10^6 \sim 10^8$ M^{-1} under physiological conditions [18, 19]. Cation-induced conformational changes are central to the target activation mechanism of EF-hand Ca^{2+} sensor protein such as centrin, and CaM [4]. The mechanism for activation of Ca^{2+} sensors involves in cation-induced structural rearrangements within each domain, which lead to the formation of large hydrophobic cavities on the molecular surface that mediate the interaction with target proteins. Binding melittin with EoCen suggested that hydrophobic patches of EoCen mainly lie in the C-terminal domain of the protein [20]. Up to now, no reports regarding the cellular functions of EoCen have been published. Papers on tuning the affinity for lanthanides of Ca^{2+} binding proteins CaM have been well done. Therefore, it can be inferred that EoCen may hold the characterization of binding with Ln ions. Indeed, our previous work has proved that Tb^{3+} may bind with EoCen, induce its conformational changes and affect the aggregation of the protein [21]. However, the interactions of other Ln ions with EoCen remain unstudied. In order to investigate this query, the C-terminal domain of *Euplotes octocarinatus* centrin (C-EoCen, 90–168 aa) was constructed, expressed and purified. Ln ions of La^{3+}, Nd^{3+}, Eu^{3+}, Gd^{3+}, Tb^{3+} and Tm^{3+} binding with C-EoCen was monitored through the difference UV–vis spectroscopy by introducing ligand xylenol orange (3,3′-bis[*N,N'*-bis- (carboxymethyl)-amino- methyl]-*o*-cresolsufonphthalein). In addition, by means of fluorescence spectroscopy and circular dichroism (CD) spectroscopy including far-UV CD and near-UV CD, the characterization of Ln ions binding with C-EoCen was studied under physiological conditions. Our results revealed the effects of Ln ions on the conformation of C-EoCen, which will shed light on the mechanism of centrin functions in the cell.

Materials and Methods

Reagents

Lanthanide oxides including La_2O_3, Nd_2O_3, Eu_2O_3, Gd_2O_3, Tb_4O_7, and Tm_2O_3 were 99.99% and purchased from Hunan in China. Lanthanide (Ln) chloride solution was prepared by dissolving lanthanide oxides in HCl. After the excess HCl was removed by heating, $LnCl_3$ was dissolved in weak acid solution, which was standardized by complexiметric titration with ethylenediamine- *N,N,N',N'*-tetra-acetic acid (EDTA) in HAc/NaAc buffer at pH 5.5.

N-2-hydroxyethylpiperazine-N-2-ethanesulfonic acid (Hepes) and 2-*p*-toluidinylnaphthalene- 6-sulfonate (TNS) were purchased from Sigma. Hepes, TNS, salts, and other chemicals utilized in protein purification are of analytical grade. 3,3′-bis[*N,N'*-bis(carbo-xymethyl)-aminomethyl]-*o*-cresolsufonphthalein (xylenol orange, XO) is of JIS special grade (SAJ, >95%).

Yeast extract, tryptone, isopropyl-β-D-dthiogalactoside (IPTG), and ampicillin (Amp^r) were purchased from Amresco Ltd. Other biochemical reagents in construction, expression and purification of protein were purchased from TaKaRa.

Protein Preparation

Construction and Cloning of C-EoCen

Recombinant C-terminal domain of *Euplotes Octocarinatus* centrin (C-EoCen) was expressed and purified as described previously [20, 21]. Using EoCen as template, C-EoCen was obtained by PCR through forward and reverse primers of 5′- CCGGGATCCATTGGATTTGATGATTTTCTTGATATTATG-3′ and 5′-CCGAAGCTTTTATTCTACAGGATCTCT-3′. The underlined sequence "GGATCC" is BamHI restriction enzyme sites. Then products were subcloned into expression vector of pGEX-6p-1. The sequence of the clone was confirmed by commercial company.

Protein Expression and Purification

After verification by DNA sequence analysis, the recombinant plasmid was transferred into *E. col.* (DE3), which was incubated at 37 °C. At an optical density of 0.6~0.8 (at 600 nm), protein synthesis was induced using isopropyl-β-D-thiogalactopyranoside (IPTG 0.8 mM) for 3.0 h. The protein was purified as a GST fusion protein using glutathione sepharose 4FF in PBS (KH_2PO_4 1.8, Na_2HPO_4 10, KCl 2.7 and NaCl 140 mM). The GST fusion proteins were then cleaved by PreScission Protease (PPase) and the cleavage protein fragments were further purified by HPLC. The purity of the intermediate and final samples was assessed by SDS-PAGE. After purification, the protein was concentrated and kept at −80 °C.

The protein C-EoCen was soluble and its concentration was measured by its absorption at 280 nm with an extinction coefficient of ε_{280}=1,400 M^{-1} cm^{-1}.

Metal Removal

To remove contaminating bound cations, the protein samples of C-EoCen were first pretreated with EDTA and then passed through a 40 cm×1 cm Sephadex G-50/G-75 column equilibrated in Hepes buffer (100 mM), at pH 7.4.

Lanthanide Affinity

The binding constants of Ln ions including La^{3+}, Nd^{3+}, Eu^{3+}, Gd^{3+}, Tb^{3+}, Tm^{3+} with C-EoCen were measured by the difference UV–vis spectra on Hewlett Packard 8453 spectrophotometer. A mixed solution of 200 μL xylenol orange (1.1 mM), 60 μL NaCl (5 M) and 1,740 μL Hepes buffer (100 mM, pH 7.4) was added to a 1 cm sample cuvette, and then Ln ions (~4.0×10^{-3} M) was added gradually to determine the absorbance of the complex Ln-XO. Xylenol orange was also titrated using the solution of Ln ions in the presence of C-EoCen as competing ligand to measure the binding constants of Ln ions with C-EoCen under the same conditions as above. During the titration, the sample was maintained at 25 °C by a jacketed cell holder connected to an external circulating water bath (Huber). To correct for dilution during each titration and to normalize the results from different titrations, the absorbance were converted to absorptivities (ε) by dividing the absorbance by the analytical concentration of xylenol orange.

Circular Dichroism Spectroscopy

Circular dichroism (CD) measurements were carried out on MOS 450 (BioLogic, France) spectropolarimeter continuously purged by N_2 and equipped with a temperature-control system. All spectra were the average of three scans with a step size of 0.2 nm and a bandwidth of 1 nm. Far-UV spectra were recorded between 195 and 250 nm using 1 mm path length quartz cells. C-EoCen was measured at concentrations of 23 μM in 2 mM Hepes at pH 7.4. Near-UV spectra were recorded between 250 and 280 nm using 1 cm path length quartz cells. The concentration of C-EoCen was kept at 196 μM in 10 mM Hepes at pH 7.4. The buffer signal was digitally subtracted using the software provided by the manufacturer. For the Ln ions titration, small aliquots of about 8 mM $LnCl_3$ solution were added to achieve Ln-to-protein molar ratios of 1:1 or 2:1. To correct for dilution during each titration and to normalize the results from different titrations, the CD data were converted to molar ellipticity by dividing the ellipticity by the analytical concentration of C-EoCen.

Interaction with Hydrophobic Probes

The Ln-dependent changes in the hydrophobic core on C-EoCen were followed by monitoring fluorescence properties of TNS as described previously on HITACHI 850 [22]. The Ln ions titrations were carried out on 6 μM metal-free C-EoCen excited with 322 nm in 100 mM Hepes and 150 mM NaCl at pH 7.4. The slit widths for excitation and emission were 5 nm. A filter with a long pass of 390 nm was used to avoid secondary Raleigh scattering. An equilibrium time of 5 min was used between each titration.

Resonance Light Scattering

Resonance light scattering (RLS) of samples was monitored by fluorescence in quartz cells of 1-cm optical path at room temperature (25 °C). The RLS was performed in 100 mM Hepes at pH 7.4 with a fluorescence spectrometer (F-2500, Hitachi, Japan), using the same excitation and emission wavelengths. Samples (1.3 μM ca.) were prepared by

gradually adding Ln ions such as La^{3+}, Nd^{3+}, Eu^{3+}, Gd^{3+}, Tb^{3+}, Tm^{3+}, into solution of proteins.

An equilibrium time of 5 min was used between each titration.

Results

Expressing and Purification of Recombinant C-EoCen

Engineered *E. col* BL21 strains of recombinant plasmid pGEX-6p-C-EoCen was cultured at 37 °C for 3~4 h to produce the corresponding proteins. Thereafter, recombinant protein was purified as a GST fusion protein using glutathione sepharose 4FF in PBS buffer. The GST fusion proteins were then cleaved by PreScission Protease (PPase) and the cleavage protein fragments with about 37% yield (Fig. S1).

Binding Constants of Ln Ions with C-EoCen

In the present paper, we introduced xylenol orange into the system. Here, xylegnol orange served as a light-emitting ligand but not indicator. Ligand of xylenol orange and C-EoCen bind competitively with Ln ions. However, there is no interaction between C-EoCen and xylegnol orange (Fig. S2). As a blank solution, xylenol orange was firstly titrated with Ln ions in 100 mM Hepes and 150 mM NaCl at pH 7.4. Through the method described previously [22], the binding constants of Ln ions with xylenol organge were calculated (Table S1). To calculate the binding constant of Ln ions with the protein, xylenol orange was also titrated with Ln ions in the presence C-EoCen under the same experimental conditions. Figure 1a shows the difference UV–vis spectra of Ln ions for example La^{3+} titration of the blank solution of C-EoCen and xylenol orange. With the addition of La^{3+}, four positive peaks at 295, 360, 520 and 605 nm and four negative peaks at 265, 320, 425 and 575 nm increased. In order to correct the dilution, the absorbance at 605 nm was converted to absorptivity by dividing the absorbance via the concentration of xylenol orange. Titration curves in the presence or absence of C-EoCen were prepared by plotting absorptivity at 605 nm versus [Ln]/[XO] for example $[La^{3+}]$/[XO] in Fig. 1b. It can be seen that an inflexion appeared at about $[La^{3+}]$/[XO]= 1.0, which confirmed 1:1 stoichiometric ratio of La^{3+} to

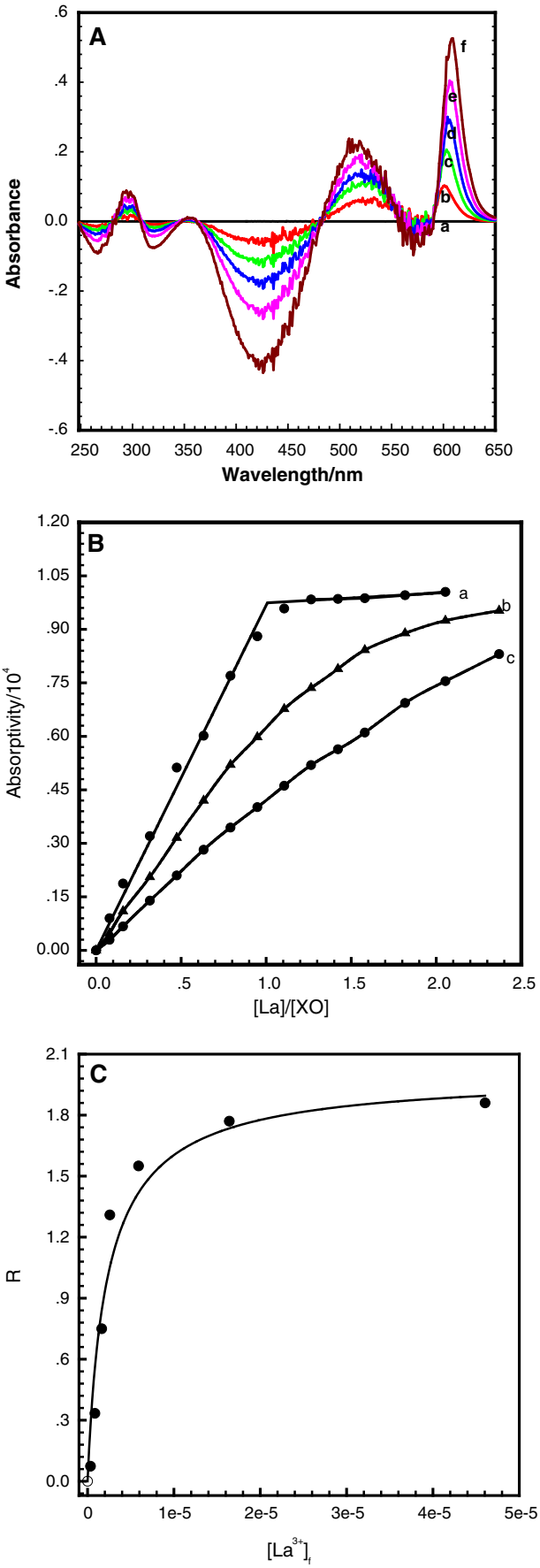

Fig. 1 **a**: Difference UV–vis spectra for the addition of La^{3+} to 2 mL mixed solution of XO (1.1×10^{-4} M) and C-EoCen (1.4×10^{-5} M) in 100 mM Hepes and 150 mM NaCl at pH 7.4. The volume of La^{3+} (3.6×10^{-3} M) is (*a*) 0 μL; (*b*) 15 μL; (*c*) 30 μL; (*d*) 45 μL; (*e*) 60 μL; (**f**) 80 μL. **b**: Titration curve for the addition of La^{3+} to the mixed solution of XO and C-EoCen in 100 mM Hepes and 150 mM NaCl at pH 7.4. Rt = [C-EoCen]/[XO]. (*a*) Rt=0, (*b*) Rt=0.96, (*c*) Rt=1.81. **c**: Fitting curve of the number R of La^{3+} bound on C-EoCen versus the free concentration of La^{3+}

xylenol orange. Comparing curve a with b and c indicated that the absorptivity of xylenol orange at given $[La^{3+}]/[XO]$ was smaller in the presence of C-EoCen than that in the absence of C-EoCen. Assuming that the decreases of absorptivity at given $[La^{3+}]/[XO]$ is attributed to the changes of La-XO to La-C-EoCen or La-C-EoCen-La. The system was described by mass balance equations for La^{3+}, XO and C-EoCen. The concentrations of La^{3+}, XO and C-EoCen can be calculated as following formulas (1)-(6):

$$r = \frac{[La]_b}{[C-EoCen]_t} = \frac{K_3[La]_f + 2K_3K_4[La]_f^2}{1 + K_3[La]_f + K_3K_4[La]_f^2} \quad (1)$$

$$[La]_f = \frac{[La-XO]}{[XO]_f} \bullet \frac{1}{k} \quad (2)$$

$$[La-XO] = [XO]_b = \frac{\Delta\varepsilon}{\varepsilon_\infty}[XO]_t \quad (3)$$

$$[XO]_f = [XO]_t - [XO]_b \quad (4)$$

$$K_3 = K_{III} + K_{IV} \quad (5)$$

$$K_4 = K_{III} \bullet K_{IV} \quad (6)$$

Where, $[La]_f$, and $[La]_b$ represent the free concentration and bound concentration of La^{3+}, respectively. $[XO]_f$ is the free concentration XO. [La-XO] represents the concentrations of complex La-XO. $[C\text{-}EoCen]_t$ is the total concentration of the protein C-EoCen. The binding constants k of La^{3+} with XO can be obtained as previously described [23]. The R is the bound La^{3+} per protein. Thus, the fitting curve of $[La^{3+}]_f$ versus R was plotted. Combined formula 5 and 6, the binding constants $\log K_{III}$ and $\log K_{IV}$ of (5.86±0.31) and (5.39±0.37) in 100 mM Hepes and 150 mM NaCl at pH 7.4 can be calculated from Fig. 1c through nonlinear fitting, respectively. These macroscopic binding constants yield the information on the pace of the successive binding steps. There are two functional metal binding sites III and IV in C-EoCen, and the affinity constants K_{III} and K_{IV} are related to each site. K_3 and K_4 represent the mean affinity constant of site III, IV of C-EoCen.

Through the same spectral method, the binding constants of Nd^{3+}, Eu^{3+}, Gd^{3+}, Tb^{3+}, Tm^{3+}, with the two binding sites on C-EoCen have been measured in 100 mM Hepes and 150 mM NaCl at pH 7.4 (Table 1). The result of Tb^{3+} with C-EoCen is consistent with the reported data [18, 19]. In addition, the binding constants of Ln ions with site IV on C-EoCen versus ion potentials of Ln ions (e/r') were plotted in Fig. 2. It can be seen that the affinity of Gd^{3+} with C-EoCen is the strongest among these rare earth ions.

Ln-Induced Conformational Changes from Circular Dichroism Spectroscopy

Circular dichroism (CD) spectra were used to examine the distribution of secondary structural elements on C-EoCen and to determine whether any changes occurred upon binding Ln ions with the protein. The far- and near-UV CD spectra of C-EoCen were shown in Fig. 3. In both apo-state and metal-bound state, the spectra are characterized by double minima peaks at 208 and 222 nm, which are indicative of a protein rich in α-helices [24]. With the additional Ln ions, such as La^{3+}, there showed a more negative spectrum, indicating that it enhanced the α-helical content of the complex (Fig. 3a). By binding with the Ca^{2+}-binding sites on C-EoCen, other Ln ions of Nd^{3+}, Eu^{3+}, Gd^{3+}, Tb^{3+}, Tm^{3+} also displays similar far-UV CD spectral properties to La^{3+} under the same experimental conditions. Binding of these rare earths ions also results in the enhancement of C-EoCen on CD signals at 208 and 222 nm. However, they exhibit different enhancement amplitudes, which may be cause by the different ion potential of Ln ions (Fig. 3b). The molar ellipticity of C-EoCen at 208 nm increases 10.3% in the La^{3+}-saturated state compared with the apo-state. Figure 3b insert displays Ln-induced secondary changes per molar C-EoCen. Gd^{3+} was more influenced on the protein conformation than other Ln ions.

As shown in Fig. 3c, the near-UV CD spectra do not, with the addition of Ln ions such as La^{3+}, display any signal from the tyrosine residue (Tyr 168) in the protein and instead display three negative signals at ~255, ~262 and ~268 nm belonging to the 4 phenylalanines residue (Phe) of C-EoCen (Table 2). Analysis of the near-UV CD spectral changes due to La^{3+}-binding indicates that the pronounced increase in asymmetry of microenvironments of Phe occurs. Also, this is indicative of changes on C-EoCen tertiary structure.

Table 1 Binding constants (K_{III} and K_{IV}) of Ln ions (La^{3+}, Nd^{3+}, Eu^{3+}, Gd^{3+}, Tb^{3+}, Tm^{3+}) with C-EoCen in 100 mM Hepes and 150 mM NaCl at pH 7.4

	La^{3+}	Nd^{3+}	Eu^{3+}	Gd^{3+}	Tb^{3+}	Tm^{3+}
$\log K_{III}$	5.26±0.37	5.98±0.41	6.68±0.52	6.91±0.57	6.75±0.34	6.64±0.24
$\log K_{IV}$	5.86±0.31	6.58±0.25	7.28±0.45	7.51±0.64	7.35±0.27	7.24±0.18

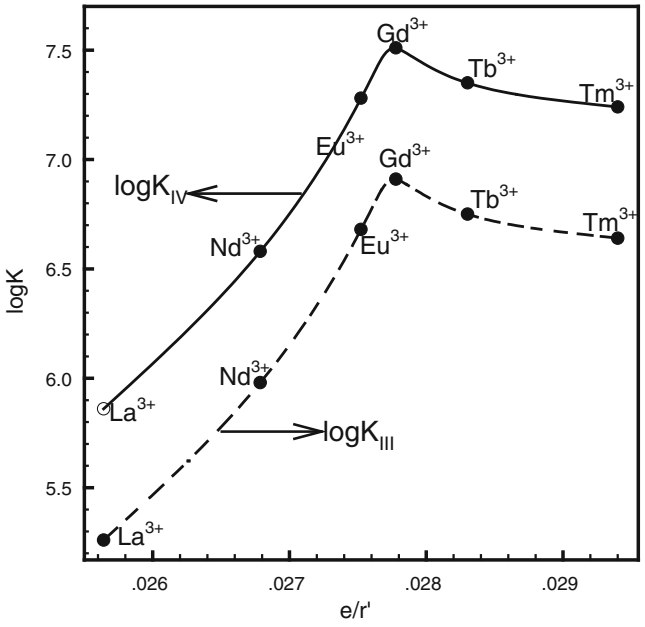

Fig. 2 The plot of logK vs eEffect of ion potential (e/r') of Ln ions

Interaction with Hydrophobic Probe

Undergoing large conformational changes is required for the trigger proteins (Ca^{2+}-modulated proteins or sensor proteins, such as CaM and troponin C) to regulate a vast number of target proteins [25, 26]. Hydrophobic fluorophore TNS is a useful probe of such conformational changes [27, 28]. Its fluorescence emission is altered when TNS binds to hydrophobic patches on the accessible surface of proteins. As shown in Fig. 4a, La^{3+} binding with C-EoCen resulted in 15-fold enhancement of fluorescence intensity and about 30 nm of blue-shift for the peak position of the hydrophobic probe TNS compared with apo-C-EoCen. Ca^{2+}-induced exposure of hydrophobic surfaces on the EF-hand Ca^{2+}-sensor proteins has been reported to be a key step in signal transduction [25]. Ln ions hold similar characterizations with Ca^{2+}. Hence, similar fluorescence intensity increase and fluorescence peak blue-shift of TNS/C-EoCen can be observed in the presence of Nd^{3+} or Eu^{3+} or Gd^{3+} or Tb^{3+} $^{+}$ or Tm^{3+}. And Gd^{3+} has the most significant effect on the conformational changes of C-EoCen (Fig. 4b). The instantaneous fluorescence changes upon binding of Ln ions suggest that holo C-EoCen adopts an open conforma-

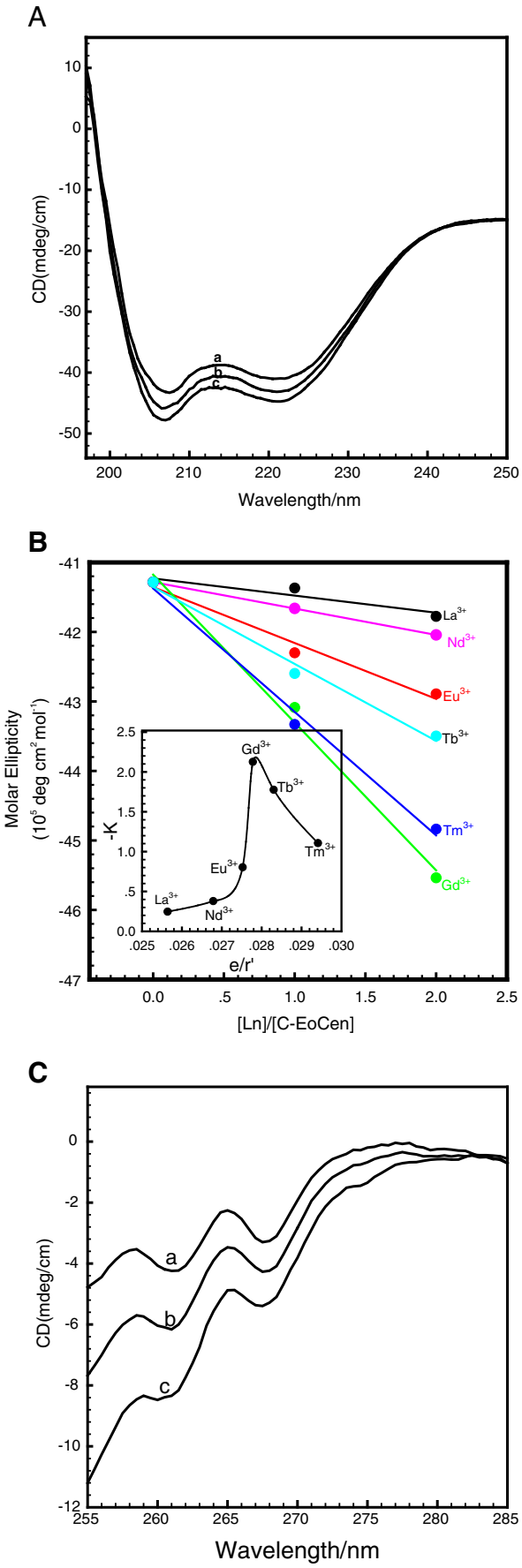

Fig. 3 **a**: Far-UV CD spectra of C-EoCen (23 μM) bound La^{3+}, the molar ratio of metal to protein is 0 (*a*), 1.0 (*b*), and 2.0 (*c*) using 1 mm path length quartz cells in 2 mM Hepes and 150 mM NaCl, pH 7.4 at 25 °C. **b**: The plots of molar ellipticity of Ln-C-EoCen against the ratio of Ln to C-EoCen. **c**: Near-UV CD spectra of C-EoCen at (196 μM) bound La^{3+}, the molar ratio of metal to protein is 0 (*a*), 1.0 (*b*), and 2.0 (*c*) using 1 cm path length quartz cells in 10 mM Hepes and 150 mM NaCl, pH 7.4 at 25 °C

Table 2 Comparison of the amino acid sequence of the two Ca^{2+}-binding sites in C-EoCen

MYIG*F*DD*F*LDIMTEK														
	E-helix	Ca^{2+}-loop												F-helix
		1	2	3	4	5	6	7	8	9	10	11	12	
	101	EF-hand III												129
IKNRDPVE	EILKAFKV*F*	**D**	**E**	**D**	**N**	**S**	**G**	**K**	**I**	**S**	**L**	**R**	**N**	LKRVAKEL
	137	EF-hand IV												165
GENLSDD	ELQAMIDE*F*	**D**	**K**	**D**	**Q**	**D**	**G**	**E**	**I**	**S**	**E**	**Q**	**E**	FLNIMKQT
SI*Y*														

Aromatic amino acid (Y and F) display in italic font and having underline

tion and Ln-loaded C-EoCen exposes more hydrophobic surface.

Resonance Light Scattering Measurement

Resonance light scattering (RLS) was used to detect the aggregated chromophores, which exhibits strong RLS signals [29, 30]. A series of fluorescence RLS was conducted at different wavelength between 250 and 600 nm to monitor the aggregation of C-EoCen in 100 mM Hepes at pH 7.4 (Fig. 5). With the addition of Ln ions such as La^{3+}, molar scattering light intensity at 366 nm increased continuously and finally reached to larger amplitude indicating the presence of large scattering particles, with sizes comparable to the observation wavelength (Fig. 5a). Similar phenomena can also be observed while added any of other rare earth (Nd^{3+} or Eu^{3+} or Gd^{3+} or Tb^{3+} $^{+}$ or Tm^{3+}) ions into the solution of C-EoCen. And these changes in RLS spectra are consistent with that from Ca^{2+}-loaded C-EoCen [31]. As a result of forming large scattering particles, the final amplitude of C-EoCen induced by Ln ions is relatively high. While EDTA was added into the above system of Ln-saturated C-EoCen in 100 mM Hepes at pH 7.4, molar RLS at 366 nm was deduced significantly, which suggested the disappearance of scattering particles (Fig. S3). Therefore, this self-assembly process is reversible. Analyzing the curves of the enhancement of resonance light scattering intensity induced by per molar protein versus ion potential (e/r') suggested that Gd^{3+} has a larger contribution to the polymerization of the protein (Fig. 5b).

Discussion

On the basis of a number of physicochemical techniques, we characterized the Ln-binding properties of the highly purified C-terminal domain of *Ciliate E. octocarinatus* Centrin (C-EoCen). Results show that C-EoCen binds one molar of Ln ions (La^{3+}, Nd^{3+}, Eu^{3+}, Gd^{3+}, Tb^{3+}, Tm^{3+}) with high affinity and one molar of Ln ions with low affinity. According to the reported data [19], site IV was assigned as high affinity site and site III was assigned as low affinity site of EoCen (Table 1). Ln-induced C-EoCen undergoes a conformational change from a closed state to an open state. At the same time, the hydrophobic patches on the surface of protein were exposed. A characteristic feature of proteins from the EF-hand superfamily is the wide diversity in the cation binding properties, including the affinity, kinetics, specificity, and cooperativity [32]. Apart from Ca^{2+}, EF-hand proteins of CaM [15], parvalbumin [33, 34], troponin C [35] may bind one molar Ln ions, at least, per molar protein at the Ca^{2+}-binding sites. Centrin belongs to the EF-hand superfamily. EoCen contains two paired canonical EF-hand motifs of helix-loop-helix in two domains, which bind two Ca^{2+} with high affinity (~10^5 M^{-1}) and two Ca^{2+} with low affinity (~10^3 M^{-1}) [19]. Besides Ca^{2+}, this EF-hand protein of EoCen can also bind with Ln ions, for example Tb^{3+}, Lu^{3+} at the Ca^{2+}-binding sites and undergoes metal ion-dependent structural transition [18, 21, 23]. Pervious results, by monitoring Ca^{2+} quenching the sensitized emission of Tb^{3+} bound with protein at 545 nm, have also indicate that Tb^{3+} shares the same binding sites with Ca^{2+} on EoCen [18]. Through the same experiments, we proved that rare earth ions of La^{3+}, Nd^{3+}, Eu^{3+}, Gd^{3+}, Tm^{3+}, as well as Tb^{3+} can bind with C-EoCen at the Ca^{2+} binding sites (Fig. S4). Having very similar ion radii and coordination numbers, Ln ions can substitute Ca^{2+} in the protein of C-EoCen. By virtue of Ln ions possessing higher charges, they exhibit higher affinities for proteins than Ca^{2+}. It can be seen from Fig. 2 that the affinities of La^{3+}, Nd^{3+}, Eu^{3+}, Gd^{3+} with C-EoCen enhanced while that of Gd^{3+}, Tb^{3+}, Tm^{3+}, with C-EoCen decreased with the increasing of ionic potential of Ln ions. Gd^{3+} displays the highest affinity with C-EoCen among these rare earth ions. At neutral conditions, Ln ions coordinate with water molecules. Parts of water molecules coordinated with Ln ions will be displaced by amino acids on the protein while Ln ions coordinate with C-EoCen. The repulsion between remainder water molecular and amino acids increased with the decrease of ionic radius of Ln ions. Therefore, the binding constants of La^{3+}, Nd^{3+},

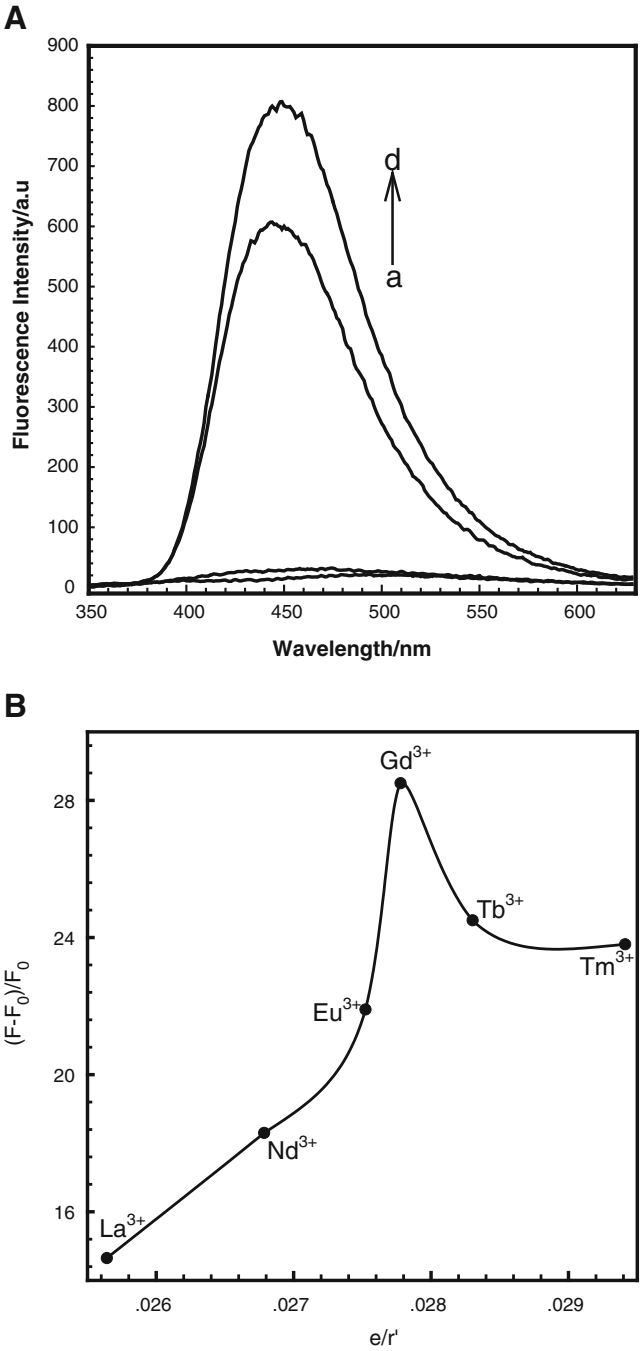

Fig. 4 **a**: Fluorescence spectra of TNS in the absence (*a*) or presence of apo C-EoCen (*b*), La^{3+}/C-EoCen=1:1 (*c*) and La^{3+}/C-EoCen=2:1 (*d*) excited with 322 nm in 10 mM Hepes and 150 mM NaCl at pH 7.4. **b**: Fluorescence intensity changes of TNS in the presence of Ln-saturated C-EoCen versus ion potential (e/r') of Ln

Eu^{3+}, Gd^{3+} with C-EoCen increased with the decrease of ionic radius. With the combination of Ln ions binding with C-EoCen, Ln ions hydrolyzed at pH 7.4. As the ionic radius smaller, the stronger hydrolysis effect of Gd^{3+}, Tb^{3+}, Tm^{3+} can be observed, which result in the affinity decrease. In addition, other factors including the size, shape of cavity constitute from the 12-residue loop of EF-hand etc. can also affect the binding Ln ions with C-EoCen. Thus, Gd^{3+} binds to the two Ca^{2+}-binding sites on C-EoCen with the highest affinities of $\log K_{III}=6.91$ and $\log K_{IV}=7.51$. In addition, the RLS and fluorescence emission of TNS on the protein also suggest such strongest effect of Gd^{3+} inducing C-EoCen

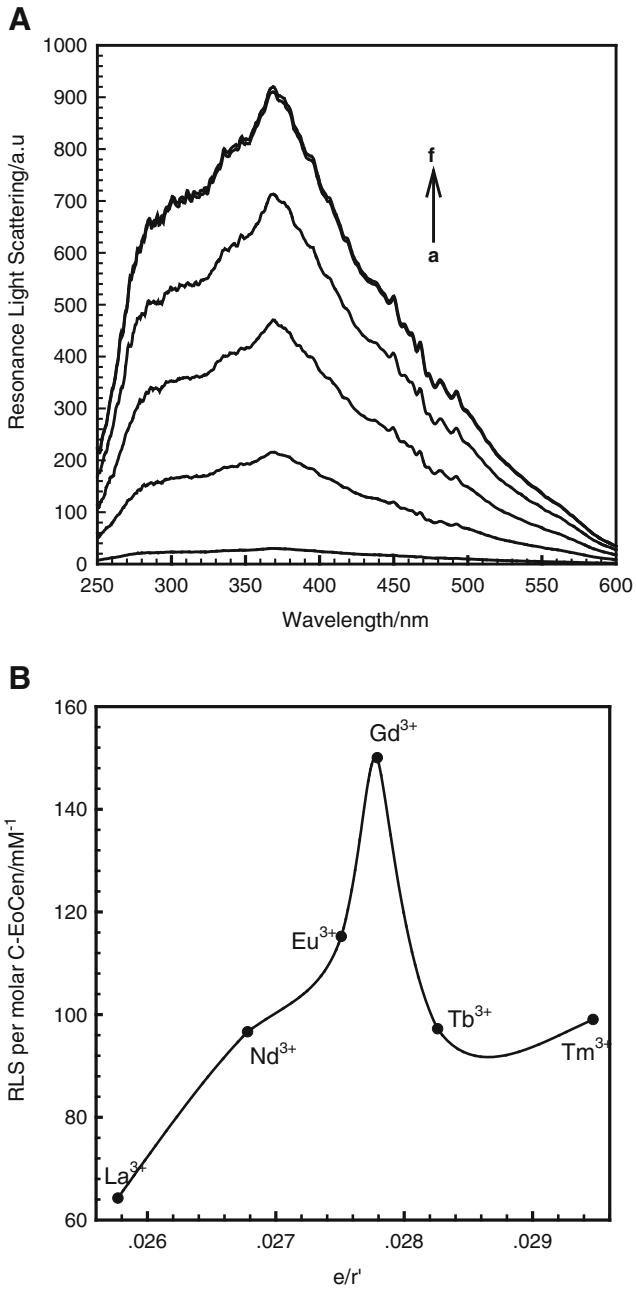

Fig. 5 **a**: Resonance light scattering spectra of La^{3+} titrating C-EoCen as a functions of the concentration of La^{3+} (micromolar) in 100 mM Hepes at pH 7.4 and room temperature. Rt' = $[La^{3+}]$/[C-EoCen] (*a*) Rt'=0; (*b*) Rt'=0.5; (*c*) Rt'=1.0; (*d*) Rt'=1.5; (*e*) Rt'=2.0; (*f*) Rt'=4.0. **b**: Plot of enhancement of resonance light scattering intensity induced by per molar protein of C-EoCen (RLS per molar C-EoCen) versus ion potential of Ln ions

conformational changes at neutral conditions. The more pronounced effects of Ln ions than that of Ca^{2+} on the conformational changes of C-EoCen probably originate from the higher affinity of lanthanides for the protein.

MTOCs are nearly ubiquitous eukaryotic organelles that regulate microtubules and their dynamics [36]. Centrin is a centrosomal protein, playing critical roles in centrosome positioning and orientation, mitotic spindle pole segregation, and in the process of microtubule severing [10]. The disorganization of microtubules and microfilaments etc. is related with canceration or apoptosis of cells in most cases [37, 38]. Paper suggested that the existence of Ln ions contribute to increase the amount and orderliness of microtubules. And, different Ln ions have maybe different effects on the stability of microtubules [39]. Hence, we infer that like CaM, the biological effects of Ln ions may, at least partially, result from the interaction of lanthanides and centrin.

Conclusions

In 100 mM Hepes and 150 mM NaCl at pH 7.4, Ln ions of La^{3+}, Nd^{3+}, Eu^{3+}, Gd^{3+}, Tb^{3+}, Tm^{3+}, can bind with C-EoCen at the Ca^{2+}-binding sites. C-EoCen binds one molar of Ln ions with high affinity and one molar of Ln ions with low affinity, and the relative affinity of site IV is higher than that of site III. By virtue of Ln ions binding with C-EoCen, the protein undergoes conformational changes from a closed to an open state. At the same time, hydrophobic patches on the surface were exposed.

Acknowledgements This work was supported by the National Natural Science Foundation of P.R. China (No. 20771068 and No. 20901048) and the Natural Science Foundation of Shanxi Province (No. 2007011024 and No. 2011021006–1). The Ph.D Programs Foundation of Ministry of Education of China (20091401110007).

References

1. Hu H, Sheehan JH, Chazin WJ (2004) The mode of action of centrin. J Biol Chem 279:50895–50903
2. Schiebel E, Bornens M (1995) In search of function for centrins. Trends Cell Biol 5:197–201
3. Salisbury JL (1995) Centrin, centrosome, and mitotic spindle ploes. Curr Opin Cell Biol 7:39–45
4. Radu L, Durussel I, Assairi L, Blouquit Y, Miron S, Cox JA, Craescu CT (2010) *Scherffelia dubia* centrin exhibits a specific mechanism for Ca^{2+}-controlled target binding. Biochemistry 49:4383–4394
5. Baum P, Furlong C, Byers B (1986) Yeast gene required for spindle pole body duplication: homology of its product with Ca^{2+}-binding protein. Proc Natl Acad Sci USA 83:5512–5516
6. Taillon BE, Adler SA, Suhan JP, Jarvik JW (1992) Mutational analysis of centrin: an EF-hand protein associated with three distinct contractile fibers in the basal body apparatus of *Chlamydomonas*. J Cell Biol 119:1613–1624
7. Sanders MA, Salisbury JL (1994) Centrin plays an essential role in microtubule severing during flagellar excision in *chlamydomonas reinhardtii*. J Cell Biol 124:795–805
8. Araki M, Masutani C, Takemura M, Uchida A, Sugasawa K, Kondoh J, Ohkuma Y, Hanaoka F (2001) Centrosome protein centrin 2/caltractin 1 is part of the Xeroderma Pigmentosum group C complex that initiates global genome nucleotide excision repair. J Biol Chem 276:18665–18672
9. Molinier J, Ramos C, Fritsch O, Hohn B (2004) Centrin 2 modulates homologous recombination and nucleotide excision repair in arabidopsis. Plant Cell 16:1633–1643
10. Fischer T, Rodriguez-Navarro S, Pereira G, Racz A, Schiebel E, Hurt E (2004) Yeast centrin Cdc31 is linked to the nuclear mRNA export machinery. Nat Cell Biol 6:840–848
11. Gonda K, Yoshida A, Oami K, Takahashi M (2004) Centrin is essential for the activity of the ciliary reversal-coupled voltage-gated Ca^{2+} channels. Biochem Biophys Res Commun 323:891–897
12. Meyn SM, Seda C, Campbell M, Weiss KL, Hu H, Pastrana-Rios B, Chazin WJ (2006) The biochemical effect of Ser167 phosphorylation on *Chlamydomonas reinhardtii* centrin. Biochem Biophys Res Commun 342:342–348
13. Hu J, Jia X, Li Q, Yang X, Wang K (2004) Binding of La^{3+} to calmodulin and its effects on the interaction between calmodulin and calmodulin binding peptide, polistes mastoparan. Biochemistry 43:2688–2698
14. Yang Q, Hu J, Yang X, Wang K (2008) Mastoparan/mastoparan X altered binding behavior of La^{3+} to calmodulin in ternary complexes. J Inorg Biochem 102:278–284
15. Ye Y, Lee H, Yang W, Shealy S, Yang J (2005) Probing site-specific calmodulin calcium and lanthanide affinity by grafting. J Am Chem Soc 127:3743–3750
16. Bertini I, Gelis L, Katsaros N, Luchinat C, Provenzani A (2003) Tuning the affinity for lanthanides of calcium binding proteins. Biochemistry 42:8011–8021
17. Wang K, Li R, Cheng Y, Zhu B (1999) Lanthanides—the future drugs? Coord Chem Rev 190–192:297–308
18. Wang ZJ, Zhao YQ, Ren LX, Li GT, Liang AH, Yang BS (2007) Spectral study on the interaction of ciliate *Euplotes octocarinatus* centrin and metal ions. J Photochem Photobiol A 186:178–186
19. Zhao YQ, Feng JY, Liang AH, Yang BS (2009) The characterization for the binding of calcium and terbium to *Euplotes octocarinatus* centrin. Spectrochim Acta A 71:1756–1761
20. Zhao YQ, Feng JY, Liang AH, Yang BS (2007) Binding of *Euplotes octocarinatus* centrin with target peptide melittin. Chinene Sci Bull 52:3216–3220
21. Duan L, Zhao YQ, Wang ZJ, Li GT, Liang AH, Yang BS (2008) Lutetium(III)-dependent self-assembly study of ciliate *Euplotes octocarinatus* centrin. J Inorg Biochem 102:268–277
22. Wang ZJ, Ren LX, Zhao YQ, Li GT, Liang AH, Yang BS (2007) Investigation on the binding of TNS to centrin, an EF-hand protein. Spectrochim Acta A 66:1323–1326
23. Liu W, Duan L, Zhao B, Zhao YQ, Liang AH, Yang BS (2010) Role of Asp37 in metal-binding and conformational change of ciliate *Euplotes ocotcarinatus* cenrin. Helth 2:262–267
24. Moncrieffe MC, Venyaminov SY, Miller TE, Guzman G, Potter JD, Prendergast FG (1999) Optical spectroscopic characterization of single tryptophan mutants of chicken skeletal troponin C: evidence for interdomain interaction. Biochemistry 38:11973–11983
25. Ikura M, Clore GM, Gronenborn AM, Zhu G, Klee CB, Bax A (1992) Solution structure of a calmodulin-target peptide complex by multidimensional NMR. Science 256:632–638
26. Zhang M, Tanaka T, Ikura M (1995) Calcium-induced conformational transition revealed by the solution structure of apo calmodulin. Nat Struct Mol Biol 2:758–767

27. McClure WO, Edelman GM (1966) Fluorescent probes for conformational states of proteins. I. mechanism of fluorescence of 2-*p*-toluidinylnaphthalene-6-sulfonate, a hydrophobic probe. Biochemistry 5:1908–1919
28. Durussela I, Blouquitb Y, Middendorpc S, Craescub CT, Cox JA (2000) Cation- and peptide-binding properties of human centrin 2. FEBS Lett 472:208–212
29. Qi WJ, Wu D, Liang J, Huang ZC (2010) Visual and light scattering spectrometric detections of melamine with polythymine-stabilized gold nanoparticles through specific triple hydrogen-bonding recognition. Chem Commun 46:4893–4895
30. Mallamace F, Micali N, Romeo A, Scolaro LM (2000) Fractal aggregation of dyes such as porphyrins and related compounds under stacking. Curr Opin Coll Interf Sci 5:49–55
31. Zhao YQ, Song L, Liang AH, Yang BS (2009) Characterization of self-assembly of *Euplotes octocarinatus* centrin. J Photochem Photobiol B 95:26–32
32. Cox J, Tirone F, Durussel I (2005) Calcium and magnesium binding to human centrin 3 and interaction with target peptides. Biochemistry 44:840–850
33. Breen PJ, Hild EK, Horrocks W, DeW J (1985) Spectroscopic studies of metal ion binding to a tryptophan-containing parvalbumin. Biochemistry 24:4991–4997
34. Breen PJ, Jonhnson KA, Horrocks WD Jr (1985) Stopped-flow kinetic studies of metal ion dissociation or exchange in a tryptophan-containing parvalbumin. Biochemistry 24:4997–5004
35. Eichmüller C, Skrynnikov NR (2007) Observation of μs time-scale protein dynamics in the presence of Ln^{3+} ions: application to the N-terminal domain of cardiac troponin C. Biomol J NMR 37:79–95
36. Ivanovska I, Rose MD (2001) Fine structure analysis of the yeast centrin, Cdc31p, identifies residues specific for cell morphology and spindle pole body duplication. Genetics 157:503–518
37. Pillai S, Bikle DD (1992) Lanthanum influx into cultured human keratinocytes: effect on calcium flux and terminal differentiation. J Cell Physiol 151:623–629
38. Xiao B, Ji YJ (1996) Item 8. State Commission of Science and Technology, Beijing, p 121
39. Soto C, Rodrigues PH, Monasterio O (1996) Calcium and gadolinium ions stimulate the GTPase activity of purified chicken brain tubulin through a conformational change. Biochemistry 35:6337–6344